REVIEW

STD-NMR: application to transient interactions between biomolecules—a quantitative approach

Jesus Angulo · Pedro M. Nieto

Abstract Saturation transfer difference NMR (STD NMR) spectroscopy is one of the most powerful NMR techniques for detection and characterization of transient (fast) receptor–ligand interactions in solution. By observing the signals of a small molecule (ligand) with spectroscopic properties suitable for high-resolution studies, irrespective of receptor size, STD NMR enables quantitative structural and affinity information to be obtained about the molecular recognition process under study. Approximately one decade after its introduction, the technique has reached maturity, and is highly robust and useful. The objective of this article is to review the current status of this powerful technique, with particular emphasis on quantitative applications, within the framework of the (bio-)chemistry of molecular recognition.

Keywords NMR spectroscopy · Saturation transfer difference NMR (STD NMR) spectroscopy · Molecular recognition · Receptor–ligand interactions

Introduction

Specific interactions between molecules in solution through non-covalent forces are the fundamental basis of molecular recognition processes. In all cases, the specificity relies on both structural and functional complementarity between the chemical groups of the interacting molecules. NMR spectroscopy has been shown to be suitable for obtaining such structural information at an atomic level, and many experiments have been developed and applied, in particular, to receptor–ligand interactions of biological relevance (Calle et al. 2011; Pellecchia et al. 2008; Pellecchia et al. 2002; Roldós et al. 2011). In general, when studied by NMR, two approaches can be distinguished:

1 observation and analysis of the receptor signals (for strong binding with $k_{off} < 1$ Hz); or
2 monitoring of the signals from the small ligand (primarily in weak binding with $k_{off} > 1$ Hz) (Lepre et al. 2004; Meyer and Peters 2003).

Saturation transfer difference spectroscopy (STD NMR) spectroscopy has become one of the most powerful and versatile NMR techniques for observing ligands, with growing applications both in academic research and in the pharmaceutical industry as a basic method in drug discovery, design, and optimization (Lepre et al. 2004; Mayer and Meyer 1999; Meyer and Peters 2003; Pellecchia et al. 2008). Originally, saturation transfer was applied to systems in moderate exchange to determine the ligand signals of the bound small molecule through the corresponding changes in intensities by magnetization transfer from the free state. (Forsen and Hoffman 1963; Hyde et al. 1980). In 1999, STD-NMR was described as an amplifying screening technique in which the saturation from the complex is detected in the averaged ligand signals, exploiting a cumulative effect in the free state (Mayer and Meyer 1999). New implementations have since been described (e.g. the use of heteronuclei either at natural abundance or in isotopically enriched samples) that extend the applicability of this robust and useful technique.

J. Angulo (✉) · P. M. Nieto (✉)
Instituto de Investigaciones Químicas, CSIC - US,
Américo Vespucio, 49, 41092 Sevilla, Spain
e-mail: jesus@iiq.csic.es

P. M. Nieto
e-mail: pedro.nieto@iiq.csic.es

Spectroscopically, the STD NMR experiment is particularly simple (Mayer and Meyer 1999). On a sample containing the receptor (large molecule with MW > 15 kDa) at low concentration (10^{-7}–10^{-8} M) and a large molar excess (1:10 up to 1:1,000) of a pool of small test compounds, two experiments are recorded (Fig. 1):

1 1D ^{1}H NMR under conditions of thermal equilibrium, the so-called reference spectrum or *off-resonance* experiment; and

2 a second ^{1}H NMR experiment, the *on-resonance* experiment, in which some protons of the receptor are selectively irradiated with low power radiofrequency for a specific period (*saturation time*) that can be varied typically in the range of several seconds.

If the irradiation conditions are adequately chosen, it is possible to saturate very efficiently only protons of the protein, but not those of the ligand. In this situation, if binding occurs, magnetization from the receptor protons will be transferred to ligand protons that are close in space in the bound state.

As in the bound state, the hydrodynamic properties of both ligand and receptor are governed by the largest

molecule (typically the receptor). Thus, transfer of magnetization in the *on-resonance* experiment leads to a significant reduction in signal intensities for the ligand (cf. negative intermolecular NOE for big, slowly tumbling molecules) (Neuhaus and Williamson 2000). For transient interactions with rapid exchange, this perturbation of ligand polarization in the bound state is transferred to the free state (bulk solution), where saturation accumulates during the saturation time of the experiment because the enthalpic relaxation (R_1) of a small molecule in the free state is much slower than the kinetic off-rate constant of the binding process ($k_{off} \gg R_1$). This process results in the macroscopic detection of (transferred) saturation on the ligand NMR signals in the spectrum (I_{sat}). Because signals are reduced in the corresponding *off-resonance* experiment (I_0), subtraction of both experiments ($I_0 - I_{sat}$) leads to positive difference signals for the molecule(s) affected by intermolecular magnetization transfer and, hence, identify binding ligands. For non-binding molecules in the mixture, intensities in both spectra remain the same and their difference spectrum cancels out. Thus, the difference spectrum exclusively contains signals of binding ligand/s while nullifying any signal of non-binding compounds (Fig. 1).
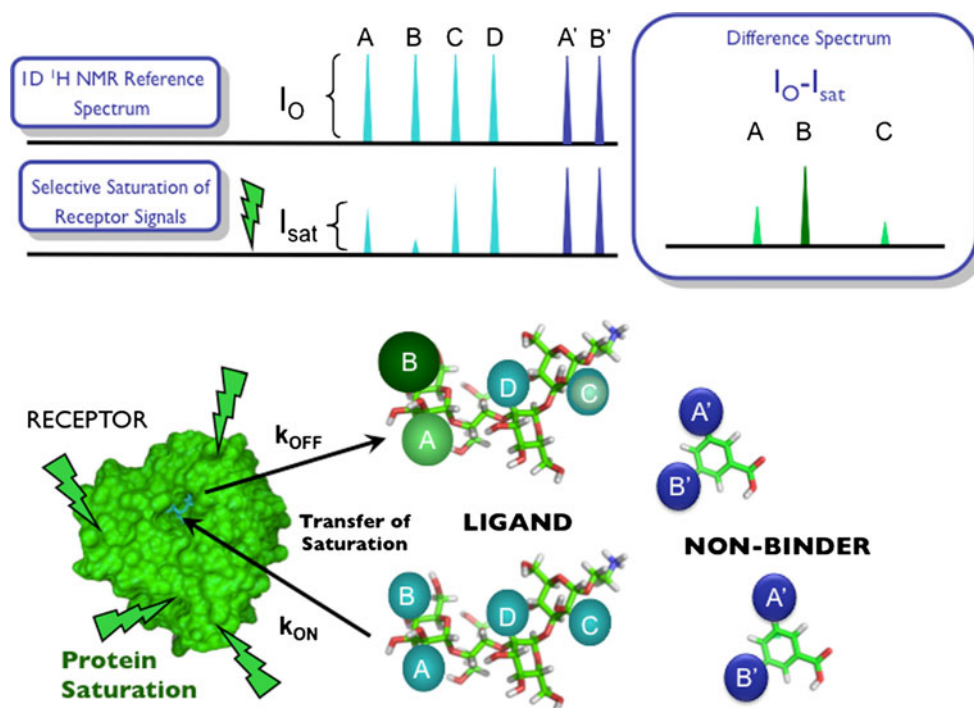

Fig. 1 Illustration of the 1D STD NMR experiment (*top*) applied to a sample containing a protein receptor in the presence of a pool of small test compounds in molar excess (*bottom*). The set-up involves recording two 1D NMR spectra: (i) a standard 1D ^{1}H NMR (*off-resonance* or *reference*) spectrum, and (ii) a 1D ^{1}H NMR spectrum with selective saturation (for a chosen saturation time) of receptor proton signals. Perturbation (saturation) of protein proton polarization can be transferred to a small molecule by intermolecular NOE if protein–ligand ^{1}H–^{1}H distances are short enough (<6 Å). Thus, transfer of saturation will only take place to molecules that transiently bind to the receptor. The difference spectrum ($I_0 - I_{sat}$, *top right*) will show only signals corresponding to the ligand(s) and signals of non-binders cancel

## Structural information on the ligand: epitope mapping

For a given ligand, not all its proton signals in the STD NMR spectrum will receive the same amount of saturation. Theoretically, the magnetization transferred from receptor to ligand protons by intermolecular NOE depends on the inverse sixth power of their distances in the bound state (Neuhaus and Williamson 2000). Thus, the distribution of saturation transferred among the different ligand protons indicates spatial proximities between the protons of the ligand molecule and the protein in the bound state (Mayer and Meyer 2001). Qualitatively, it can be assumed that stronger intensity of a ligand signal in the STD NMR spectrum indicates closer interproton distances between that ligand proton and the receptor surface in the bound state.

This figure can be analyzed in a very straightforward way, at least semi-quantitatively, by comparing the relative percentages of saturation received by the different ligand protons. This is done by normalizing all the measured STD signals ($I_0 - I_{sat}/I_0$) against the most intense signal, which is arbitrarily assumed to be 100% (Mayer and Meyer 2001). In this way, the resulting percentage STD values

represent a sort of map of the ligand—protein contacts in the bound state, delineating which chemical moieties of the ligand molecule are key for molecular recognition by the receptor (group epitope mapping, for an example see Fig. 2 bottom). Qualitatively, it can be concluded that protons with relative STD values close to 100% belong to parts of the ligand that are very intimately recognized by the receptor binding-pocket, and hence must be regarded as important for the interaction.

All STD intensities depend on the duration of radiofrequency irradiation of the protein (saturation time), and the extent of saturation transferred to the ligand protons generally increases with this time (Fig. 2 top) (Mayer and Meyer 1999, 2001). This build-up of saturation is limited by enthalpic relaxation (R_1) of saturated ligand molecules in the free state that counteracts further accumulation of STD intensity through more saturated ligand molecules dissociating from the protein binding pocket (plateau of the build-up curve, Fig. 2 top). The ligand group epitope mapping by STD intensities is typically obtained for a given saturation time (normally of the order of seconds). Ideally, epitope information would not depend on the chosen saturation time. However, significantly different R_1

Fig. 2 STD build-up curves for binding of the sugar nucleotides UDP-Gal (**1**) and UDP-Glc (**2**) to the galactosyltransferase enzyme GTB (Angulo et al. 2006). *Different colors* indicate different protons, and *different symbols* are used for the two ligands (*circles*: UDP-Gal; *triangles*: UDP-Glc). Below are shown the binding epitopes of both ligands (derived from the initial STD slopes), in which the protons with highest relative STD and, thus, the closest proximity to the receptor are highlighted in *red*. Interestingly, both ligands are recognized in the same manner, although the enzyme is specific for transfer of the Gal moiety
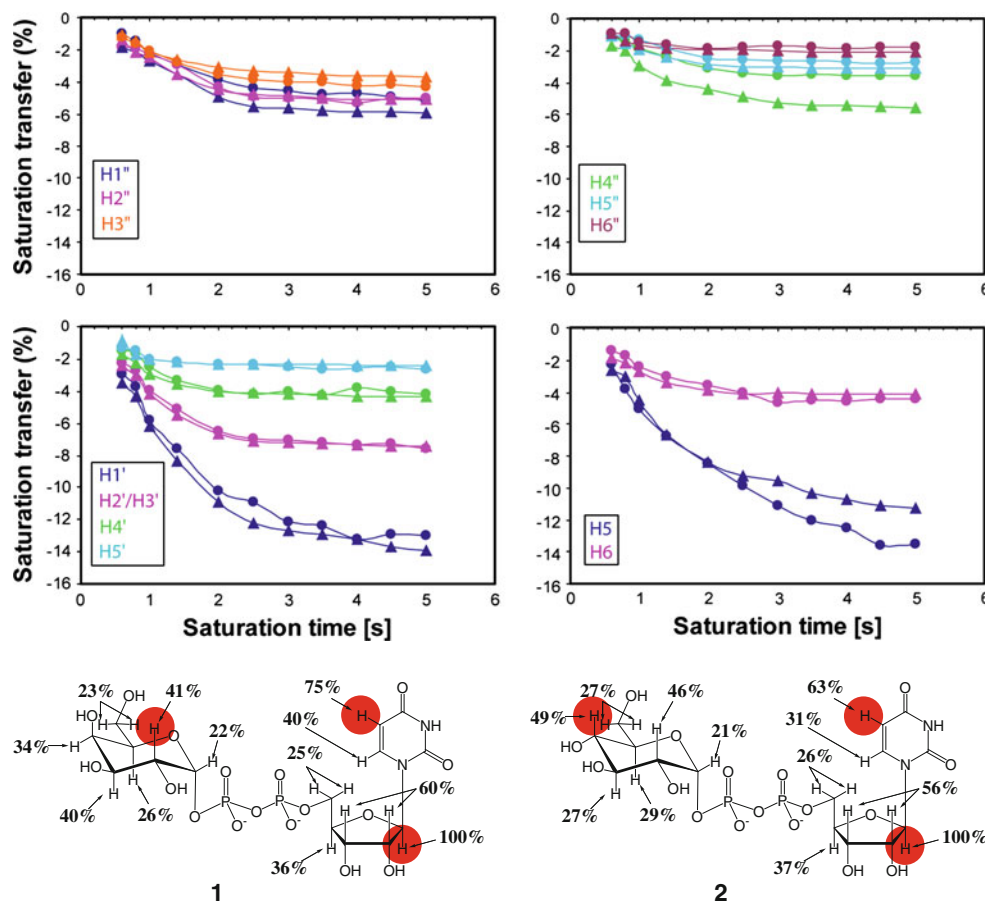
relaxation rates of the ligand protons can produce artifacts in the epitope definition. Specifically, protons with slower R_1 relaxation enable more efficient accumulation of saturation in solution such that their relative STD intensity and, thus, proximity to the binding pocket may be largely overestimated at long saturation times. The final effect on the structural information depends on several factors, e.g. on differences in ligand proton R_1 relaxation rates, in the extent of saturation received in the first place, and on the kinetics of the molecular interaction. Because all these artifacts are consequences of differences in the ability to accumulate saturation in the free state, a way to cancel them is to derive STD intensities close to zero saturation time, when virtually no accumulation of saturated ligand occurs. In addition, another biasing effect that would be minimized by using initial build up rates is the intramolecular spin diffusion within the bound state. To obtain the initial slopes, Mayer and James (2004) proposed fitting the experimental build-up curves to the monoexponential function:

$$STD(t_{sat}) = STD^{max} \cdot (1 - \exp(-k_{sat} \times t_{sat})),$$

where $STD(t_{sat})$ is the observed STD intensity, STD^{max} is the asymptotic maximum of the build-up curve, t_{sat} is the saturation time, and k_{sat} is a rate constant related to the relaxation properties of a given proton that measures the speed of STD build-up. k_{sat} and STD^{max} are derived by least-squares fitting, and the initial slope of the curve is obtained as:

$$dSTD/dt(0) = STD^{max} \cdot k_{sat}.$$

An example of ligand group epitope mapping by STD NMR is shown in Fig. 2, where the molecular recognition of two ligands (UDP-Gal and UDP-Glc) by the human blood group B galactosyltransferase (GTB) was analyzed (Angulo et al. 2006). From the STD build-up curves, initial slopes were calculated to identify the ligand epitopes (Fig. 2 bottom). The map of relative saturation transfer to the ligand indicates that both ligands are recognized in the same way by the enzyme, with both six-membered sugar rings (hexopyranose) making close contacts with the protein binding pocket. Interestingly, differential recognition of both ligands by the galactosyltransferase enzyme does not occur, although only the galactose ring is efficiently transferred in the presence of the acceptor ligand (Angulo et al. 2006).

The number of biochemical STD NMR applications for detection and characterization of transient receptor–ligand interactions has steadily increased in the last decade. Initially focused on biologically relevant transient protein–carbohydrate interactions (Bernardi et al. 2004; Jimenez-Barbero and Peters 2002; Maaheimo et al. 2000; Vogtherr and Peters 2000), STD NMR spectroscopy has also been

successfully used to characterize interactions between proteins and peptides (Megy et al. 2005; Neffe et al. 2006, 2007; Wagstaff et al. 2010), microtubuli and stabilizing agents (Canales et al. 2008), nucleic acids and ligands (Di Micco et al. 2006; Martin et al. 2005; Mayer and James 2002, 2004; Peñalver et al. 2011; Souard et al. 2008), proteins (by use of appropriate spy probes) (Blobel et al. 2008), viruses and ligands (Haselhorst et al. 2008; Rademacher et al. 2011; Rademacher et al. 2008; Rademacher and Peters 2008), to identify initial hits from combinatorial libraries (Caraballo et al. 2010; Ribeiro et al. 2010), or to study self-association processes of amiloidogenic peptides (Huang et al. 2008). A step further in biochemical applications has been the performance of "in-cell STD NMR", in which the molecular recognition of ligands by extracellular membrane proteins is studied directly by using intact cells, omitting the laborious steps of target purification and concentration. Seminal works by the laboratories of Jimenez-Barbero (Mari et al. 2005) and Meyer (Claasen et al. 2005) used this approach to characterize the interactions of the receptor DC-SIGN in K562-CD209 cells with oligomannoside ligands, and a pentapeptide with the integrin $\alpha II\beta 3$ in human platelets, respectively. Moreover, the latter work led to the development of a new "double difference" approach of the technique (STDD NMR), which has subsequently been applied to other biochemical receptor–ligand interactions of interest (Assadi-Porter et al. 2008; Claasen et al. 2005; Haselhorst et al. 2007; Pereira et al. 2009). This approach consists in recording two STD NMR experiments in parallel in two independent samples both containing the receptor, but only one with ligand added. The STDD spectrum corresponds to the double difference which cancels out spurious signals from other recognition events (Claasen et al. 2005).

Although one important advantage of the technique is that it does not require any kind of labeling on any of the interacting partners, STD NMR spectroscopy can benefit from the use of isotopic labeling of either protein or ligand. For instance, ^{15}N-GS STD experiments have been developed for ^{15}N-labeled proteins with unfavorable spectroscopic characteristics (e.g. signal overlap with the ligand) for the standard methodology, and have been successfully applied to small proteins (10–15 kDa), and proteins with enhanced internal dynamics (e.g., intrinsically disordered proteins) (Kover et al. 2007, 2010). For the ligand, isotopic labeling with ^{13}C has enabled application of edited/filtered experiments to resolve overlap problems, e.g. to determine the affinities of a series of chemically homologous compounds (Feher et al. 2008). Further STD NMR experiments have been developed to observe STD intensity on ^{19}F or ^{13}C nuclei within the ligand molecules that derives either directly from heteronuclear transfer from receptor protons or indirectly from homonuclear transfer to ligand protons

with subsequent intramolecular relay to the observed heteronucleus (via scalar coupling) (Diercks et al. 2009; Räuber and Berger 2010). Such STD techniques are of major interest for ligands with massive signal overlap, complex multiplet splittings from extensive homonuclear J_{HH} coupling, or in the presence of a large excess of non-deuterated compounds (e.g., water, buffer).

Quantitative STD NMR CORCEMA-ST

The theoretical framework for the quantitative analysis of STD NMR intensities (CORCEMA-ST) has been developed by Rama Krishna (Jayalakshmi and Krishna 2002). It is based on a modification of the CORCEMA (complete relaxation and conformational exchange matrix) theory that was originally developed for transferred-NOE experiments, (Moseley et al. 1995) and enables the prediction of STD intensities from the Cartesian atomic coordinates of the ligand–receptor complex. A schematic diagram of the model used by CORCEMA-ST is shown in Fig. 3.

In this model, two molecules (the ligand, L, and the receptor protein, P) are in rapid exchange between their free and bound states. Receptor protons P2 are directly saturated by selective irradiation. This non-equilibrium polarization then spreads from P2 to all other receptor protons P1 via *intra*molecular spin diffusion, and further to the protons of a bound ligand via *inter*molecular NOE. If dissociation occurs fast enough (cf weak binding regime with $k_{off} \gg 1/t_{sat}$), enough saturated ligand molecules accumulate in solution during the saturation time to yield a detectable STD signal (observed on the free ligand species). On the basis of this kinetics model, CORCEMA-ST can predict theoretical ligand STD intensities from a given molecular model of the protein–ligand complex if specific system properties are known (e.g., dissociation constant, k_{off}, rotational correlation times of the receptor and ligand).

In this way, CORCEMA-ST is a valuable tool for the quantitative structural interpretation of experimental STD NMR data. Experimental STD build-up curves can, thus, be compared with predictions for a model of the complex that could be obtained by use of different techniques (e.g., X-ray crystallography, NMR, docking simulations). For the matrix calculations, the Cartesian coordinates of all ligand protons and protein protons within a given cutoff distance from these are considered. How well the molecular model reproduces the experimental NMR data can be quantified by the so-called R-NOE factor:

$$R\text{-NOE} = \sqrt{\frac{\sigma W_k (STD_{exp,k} - (STD_{cal,k})^2}{\sigma W_k (STD_{exp,k})^2}}$$

where $STD_{exp,k}$ and $STD_{cal,k}$ are the experimental and calculated STD intensities, respectively, of proton k. A lower R-NOE factor indicates better fit between experimental and theoretical data and, thus, better appropriateness of the chosen structural model of the complex. In this way, different structural models derived, e.g., from different docking runs can be ranked according to how well they explain the experimental STD NMR data. Figure 4 summarizes an STD NMR study of the molecular recognition of oligomannoside ligands by the anti-HIV-1 antibody 2G12 (Enríquez-Navas et al. 2011). The complexes of 2G12 with a disaccharide and tetrasaccharide were obtained from published X-ray data, and the complex with a trisaccharide from docking simulations. From these structural models the theoretical STD intensities were predicted by CORCEMA-ST, and the resulting low R-NOE factors confirmed that the binding modes of the ligands in solution were similar to those observed in the solid state Calarese et al. 2003, 2005) (Fig. 4).

Krishna and coworkers have also demonstrated that the R-NOE factor can be used as a scoring function to drive a conformational search for the ligand bound in the receptor's binding pocket (Jayalakshmi and Krishna 2004). In this procedure (SICO: STD Intensity Restrained CORCEMA Optimization), after identifying a good starting structure with low R-NOE, the global energy minimum of the ligand in the bound state can be determined by optimizing some key torsion angles via simulated annealing driven by the minimization of the R-NOE factor. The geometry of the ligand inside the binding pocket is, thus, refined by use of experimental STD NMR data (Jayalakshmi et al. 2004; Jayalakshmi and Krishna 2005).

The kinetics of the transient ligand-receptor interaction is implicitly included in the matrix calculations, because one of the main mechanisms for saturation transfer is chemical exchange (Fig. 3) between bound and free states
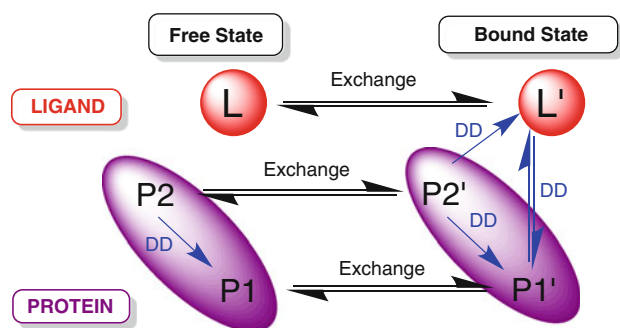

Fig. 3 Two-states kinetics model for the development of CORCEMA-ST theory to predict the STD values from Cartesian co-ordinates of the complex (bound state), and the receptor and ligand (free state). Saturation starts by selective irradiation of receptor protons P2, and is then transferred by either chemical exchange (*black arrows*), or dipole–dipole cross-relaxation (NOE, *blue arrows*)
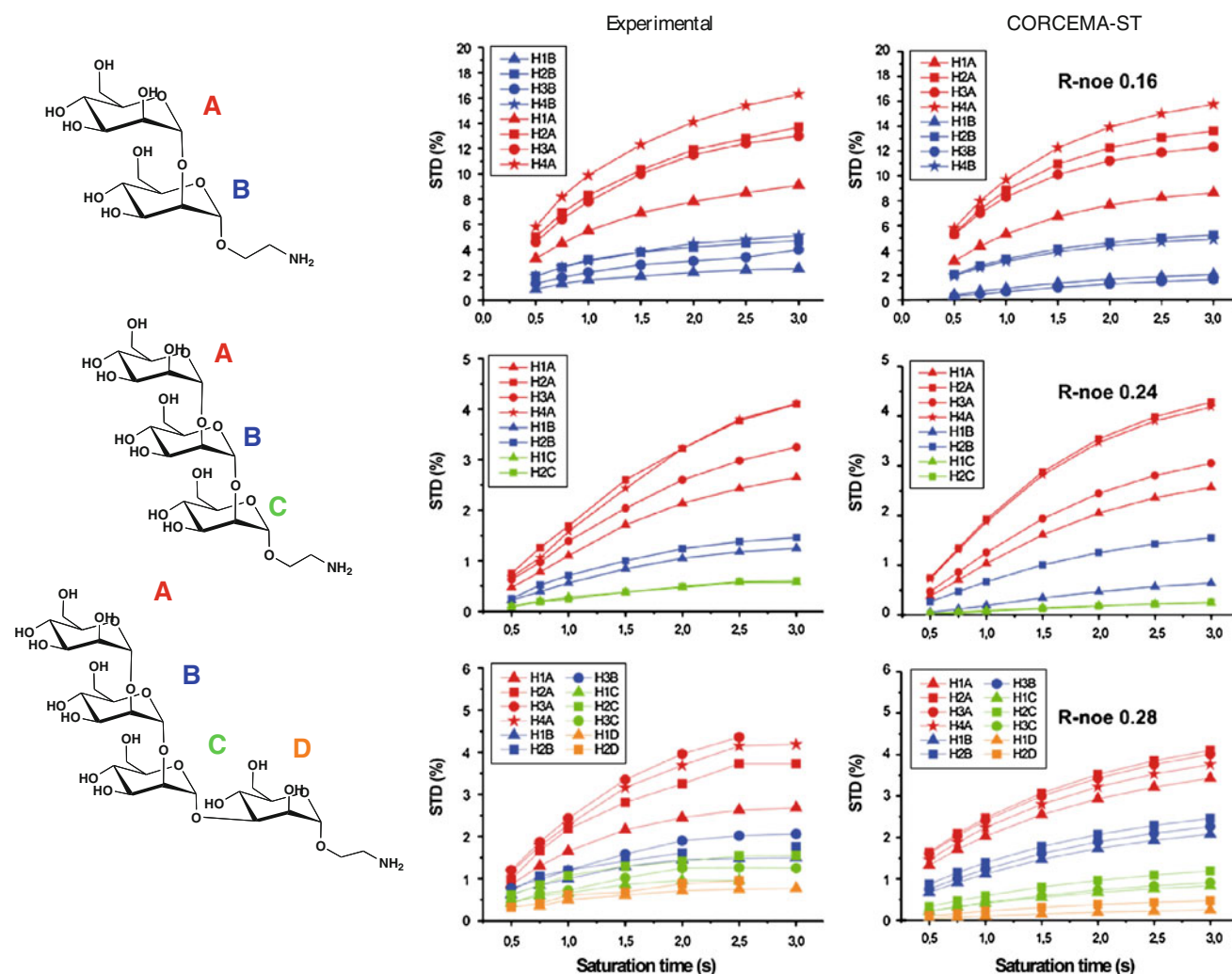
Fig. 4 Molecular recognition of linear oligomannosides by the anti-HIV-1 2G12 antibody, studied by STD NMR in solution. Comparison of experimental STD build-up curves with predictions from CORCEMA-ST based on X-ray (di and tetra-mannoside) or docking (trimannoside)-derived structural models. The excellent agreement in all cases corroborates the similarities of the (modeled) complex structures in solution and the solid state

(Jayalakshmi and Krishna 2002). Thus, results from CORCEMA-ST calculations strongly depend on kinetics. Indeed, if the complex structures of different ligands of a protein are known, their differences in affinity (and, hence, in kinetics) must be reflected in the STD NMR data, and can be inferred from quantitative CORCEMA-ST calculations. In the study of ligand recognition by human blood group-B galactosyltransferase (GTB), a series of CORCEMA-ST calculations using known complex structures and variable dissociation constants (k_{off}) revealed intrinsic differences in kinetics for the binding of donor and acceptor substrates (Fig. 5) (Angulo et al. 2006). The acceptor (H-antigen disaccharide) binds the enzyme with a k_{off} that is 10 to 10,000 times higher than that of the donor (UDP-galactose).

Determination of binding constants of transient protein–ligand interactions from the initial growth rates of STD amplification factor

STD amplification factor

The STD NMR intensity reflects the concentration of ligand-receptor complex present in solution (Mayer and Meyer 1999; Meyer and Peters 2003). Mayer and Meyer proposed a conversion from observed experimental intensities ($I_0 - I_{sat}/I_0$) to STD amplification factors (STD-AF) (Mayer and Meyer 2001), by multiplying the observed STD by the molar excess of ligand over protein (ε).

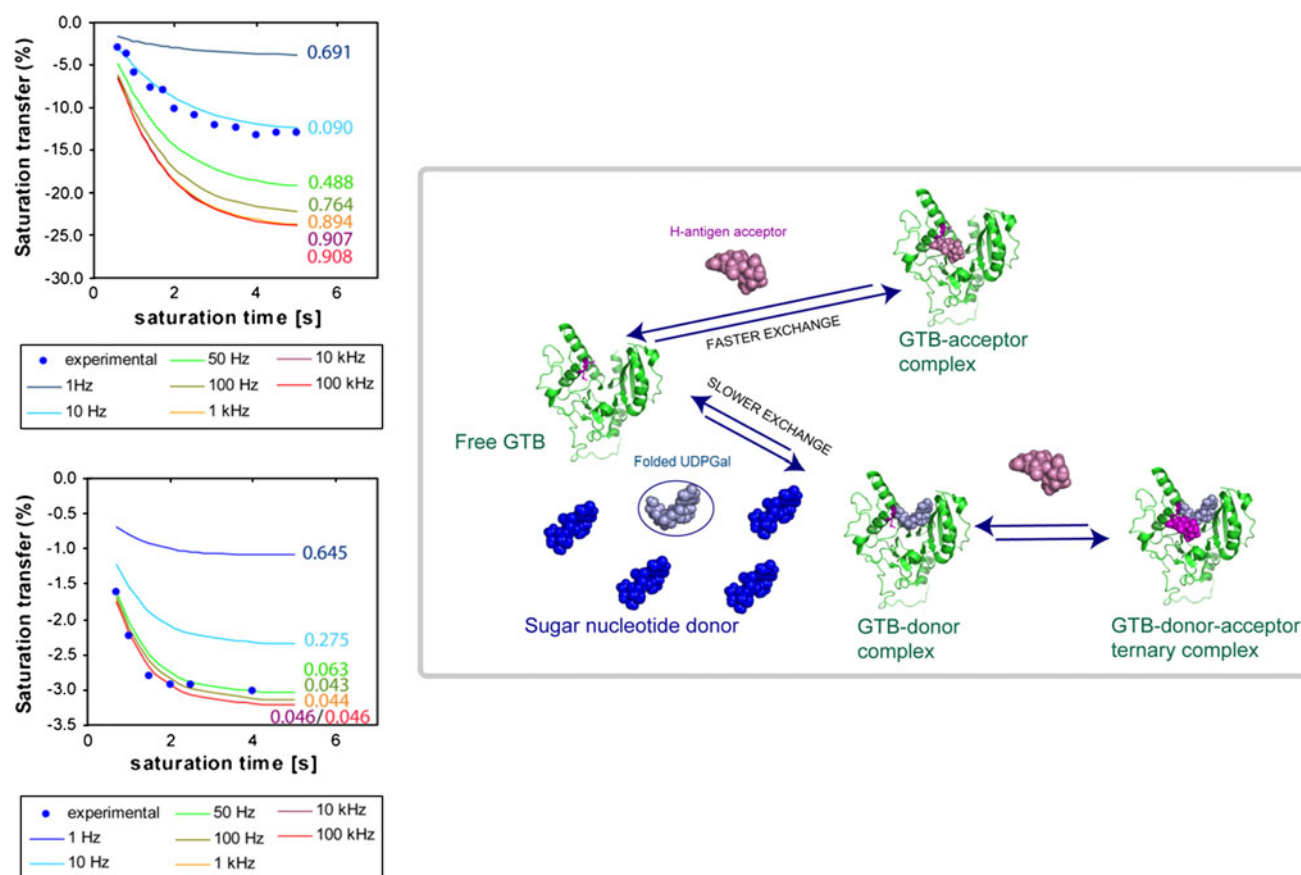$$STD - AF = \varepsilon(I_0 - I_{sat})/I_0 = \varepsilon\eta_{STD}$$

Fig. 5 STD NMR data reveal different kinetics of the binding of donor and acceptor ligands to the galactosyltransferase enzyme GTB (Angulo et al. 2006). The most intense STD signals of donor (UDP-Gal) and acceptor (H-antigen) were compared with CORCEMA-ST predictions from models of the complex for variable dissociation rates (k_{off}). The best fits were obtained for $k_{off} = 10$ Hz for UDP-Gal, and ca. 10^2–10^5 Hz for H-antigen. The *right-hand side* shows the model for a sequential mechanism, in which faster exchange of the acceptor makes it more likely that, in order for the ternary complex to form, the UDP-Gal donor is first bound to the enzyme

This converts the STD intensity, which depends on the fraction of bound ligand, into a factor (STD-AF) that is a function of the fraction of bound protein. Thus, the evolution of the STD-AF along a ligand titration series enables construction of a saturation curve in the form of an association isotherm. Such curves can be adjusted to a Langmuir equation:

$$f_{p'} = \frac{L}{K_D + [L]}$$

where $f_{p'}$ is the fraction of bound protein, [L] is the unbound ligand concentration, and K_D is the dissociation constant. The value of K_D results from the mathematical fit of the experimental curve.

In various cases, however, apparent K_D values obtained from STD NMR titrations have been shown to depend strongly on experimental conditions (e.g., saturation time, relative concentration of species, monitored proton). As an example, Fig. 6 shows four association curves (binding isotherms) obtained by use of different saturation times (1, 2, 3, and 4 s) for the interaction between the disaccharide ligand chitobiose and the lectin *wheat germ agglutinin* (WGA). These curves represent the experimental STD amplification factors normalized to their respective plateau values, enabling easier comparative analysis. This figure reveals that apparent K_D values increase monotonically with saturation time (i.e., a higher ligand concentration is needed to reach semisaturation of the protein's binding pocket; see inset in Fig. 6). Similarly, other factors, for example receptor concentration, signal intensity etc. have been demonstrated to have similar effects (Angulo et al. 2010).

The origin of such discrepancies was found to be fast ligand rebinding in solution, by which a previously saturated ligand molecule returns to the complex (bound state) before its perturbed polarization (cf saturation) has completely relaxed back to equilibrium (Angulo et al. 2010). Thus, accumulation of saturated ligand in solution during the saturation time and, thus, the observed bulk STD signal is significantly reduced when the lifetime τ_{free} of the free
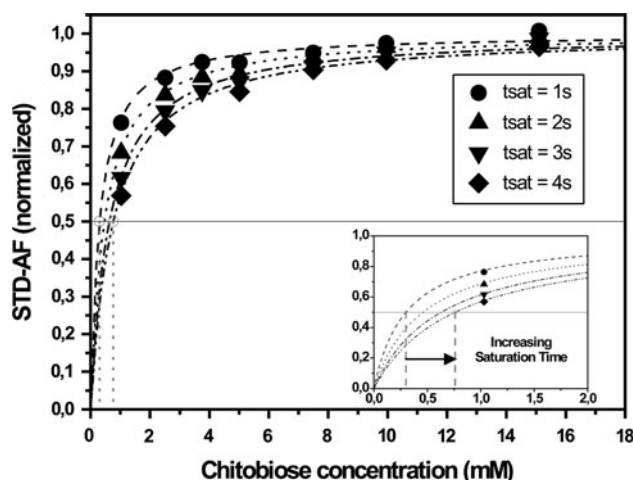
Fig. 6 Effect of STD NMR saturation time on apparent affinities of transient protein–ligand interactions (Angulo et al. 2010). The data show normalized STD-AF values for titration of the disaccharide chitobiose with the protein receptor WGA (lectin). *Different symbols* correspond to different saturation times. K_D corresponds to the ligand concentration producing a STD-AF value of 0.5. The apparent K_D increases monotonically with saturation time (*inset*)

Fig. 7 Effect of increasing the protein concentration (and, thus, the fraction of bound ligand) on the determination of K_D by STD NMR titrations (Angulo et al. 2010). The isotherms show (normalized) STD-AF values of the ligand L-tryptophan during a titration to the receptor BSA, using two different concentrations of the protein (20 μM, *light stars*, or 60 μM, *dark stars*). The increase in protein concentration leads to an increase in the apparent K_D (i.e., the ligand concentration producing an STD-AF = 0.5)

state is shorter than the T_1 relaxation time of the proton considered because of incomplete polarization recovery in the free state. The probability of such fast rebinding processes is significant for high fractions of bound ligand (for estimation under typical STD NMR conditions see supporting information of the reference Angulo et al. (2010)). This means that the strongest effects will be observed for low ligand-to-protein ratios, as typically found during the initial steps of a titration series (starting at the lowest ligand concentration). This dependence on the fraction of bound ligand also explains why such artifacts in K_D determination are stronger for systems with larger affinity (the biases typically increase from mM to μM interactions), and for titrations with larger protein concentrations (Fig. 7).

After careful study of the artifacts introduced by the different experimental conditions of the STD NMR experiment, it was concluded (Angulo et al. 2010) that:

1 the value of K_D obtained by STD NMR spectroscopy is always greater than, or equal to, the true thermodynamic value $\left(K_D^{app} \geq K_D^{real}\right)$, i.e. STD NMR data tend to *under*estimate affinities;
2 the bias introduced is greatest for ligand protons with the largest STD intensities; and
3 the deviations are exacerbated for larger protein concentrations.

Conclusions 2 and 3 indicate that attempts to improve the sensitivity of the experiment (e.g., by focusing on the most intense STD signals, or using higher protein concentrations) will negatively affect the accuracy of the
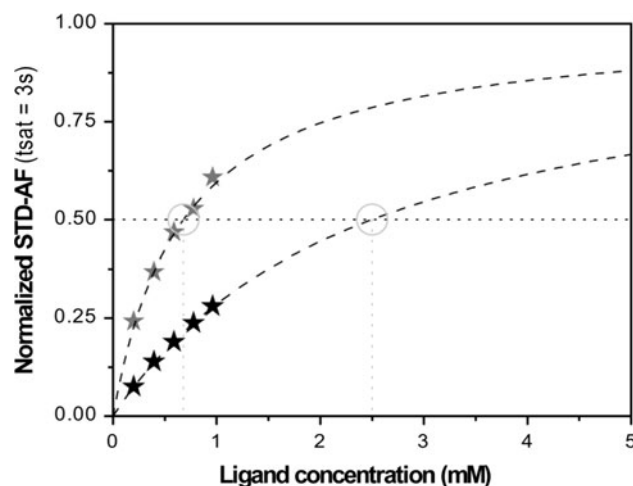
derived K_D (i.e. leading to its *over*estimation). On the other hand, conclusion 1 tells us that STD NMR titrations at least yield upper K_D (i.e., lower affinity) limits for a given ligand.

The accurate determination of dissociation constants requires the removal of all effects from fast protein–ligand rebinding in solution. Because these effects are related to the accumulation of saturated ligand in the bulk solution, they are minimized as τ_{sat} approaches 0. As for determination of ligand epitopes, this requires determination of the initial slopes of the build-up curves of STD-AF values with the saturation time.

The procedure for exact K_D determination (Angulo et al. 2010) thus involves recording a τ_{sat}-dependent STD-AF build-up curve for each ligand concentration (instead of just one STD NMR experiment at a single saturation time, as suffices for epitope mapping), then extracting the initial slopes (STD-AF$_0$):

$$\lim(t_{sat} \to 0)[d/dt\,(STD - AF)] = k_{sat}STD - AF_{max}$$
$$= STD - AF_0 = K_D.$$

Next, the binding isotherms are obtained by representing STD-AF$_0$ graphically as a function of the added ligand concentration. Finally, the K_D value is obtained by fitting to a Langmuir equation. The method is summarized in Fig. 8 and has been thoughtfully described (Angulo et al. 2010).

This new procedure cancels the artifacts from fast ligand rebinding, and yields the most accurate K_D values from STD NMR titration experiments. To illustrate the benefits of the method, Fig. 9 shows the variation of apparent K_D determined

(I)

$$STD\text{-}AF_0 = STD\text{-}AF_{max} \cdot (1-\exp(-k_{sat} \cdot t_{sat}))$$

$$STD\text{-}AF_0 = STD\text{-}AF_{max} \times k_{sat}$$

(II)

Ligand concentration [mM]	STD-AF$_{max}$	k$_{sat}$ [s^{-1}]	STD-AF$_0$ (STD-AF$_{max}$ × k$_{sat}$)
0.2	6.8 (± 0.2)	0.68 (± 0.04)	4.6 (± 0.4)
0.4	12.3 (± 0.7)	0.44 (± 0.05)	5.5 (± 0.9)
0.6	16 (± 1.0)	0.43 (± 0.07)	7.0 (± 1.5)
0.8	21 (± 1.0)	0.34 (± 0.04)	7.1 (± 1.2)
1.0	25 (± 1.5)	0.30 (± 0.03)	7.2 (± 1.5)

(III)

$$y = B_{max} * x / (K_D + x)$$

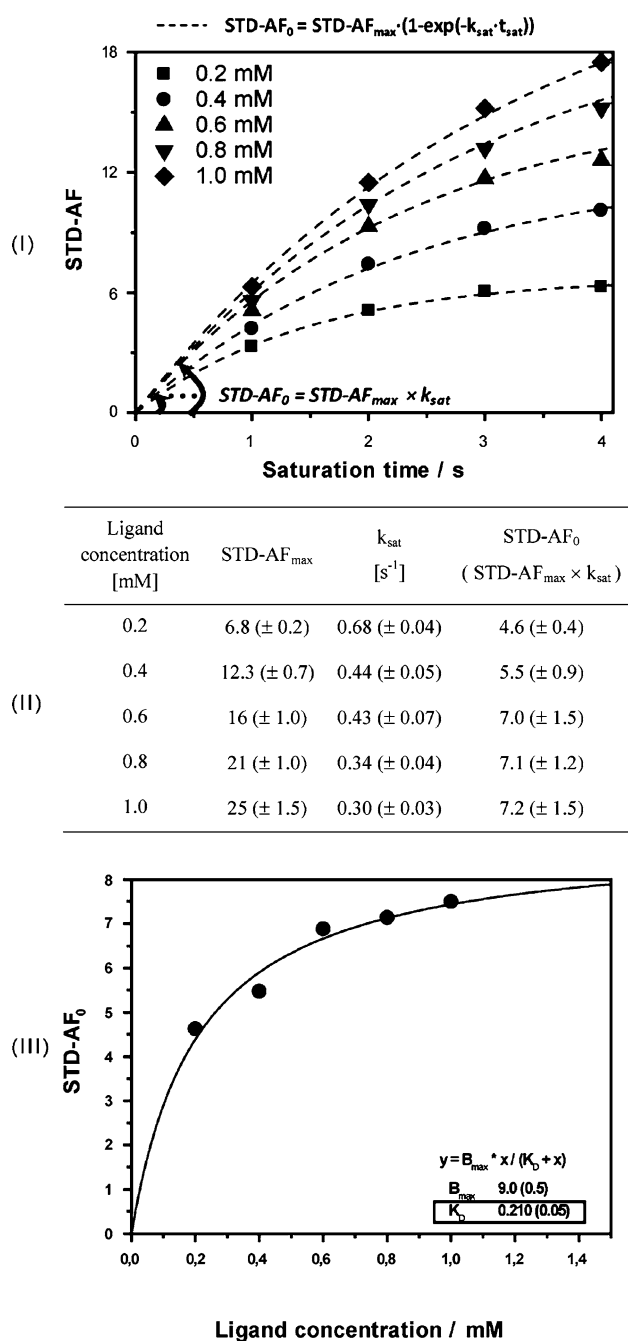B$_{max}$ 9.0 (0.5)
K$_D$ 0.210 (0.05)

Fig. 8 Approach used to derive accurate K_D values from STD NMR data, shown for L-tryptophan binding to BSA (Angulo et al. 2010). The procedure includes the following steps: (I) For each ligand concentration, a build-up curve of STD-AF values is obtained for different saturation times. (II) Each curve is mathematically fitted to obtain the initial build-up slopes STD-AF$_0$ = STD-AF$_{max}$ × k_{sat} (last column). (III) These STD-AF$_0$ values are plotted against the ligand concentration, yielding a Langmuir isotherm from which the true dissociation constant K_D can be derived (by mathematical fitting)

by STD NMR from a titration of the amino acid L-tryptophan with the protein bovine serum albumin (BSA), as a function of the saturation time and for different ligand protons. The apparent values, which grow monotonically with saturation
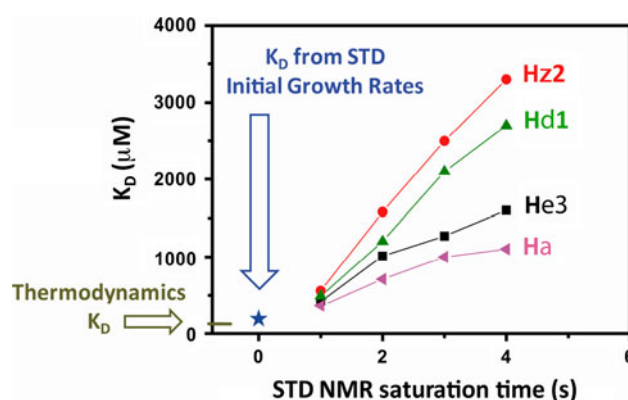

Fig. 9 Comparison of (apparent) K_D values derived from STD NMR data by different approaches. The apparent K_D obtained for the L-tryptophan—BSA system is represented as a function of the saturation time, and for different ligand protons monitored in the experiments. The K_D obtained from initial STD-AF growth rates is closest to the thermodynamical K_D constant, and is the value towards which all apparent K_D approach as the saturation time tends to zero

time and STD intensity of an observed proton, systematically converge towards the thermodynamical value at the limit of zero saturation time, which can be obtained by using the procedure of STD-AF initial growth rates (Fig. 9).
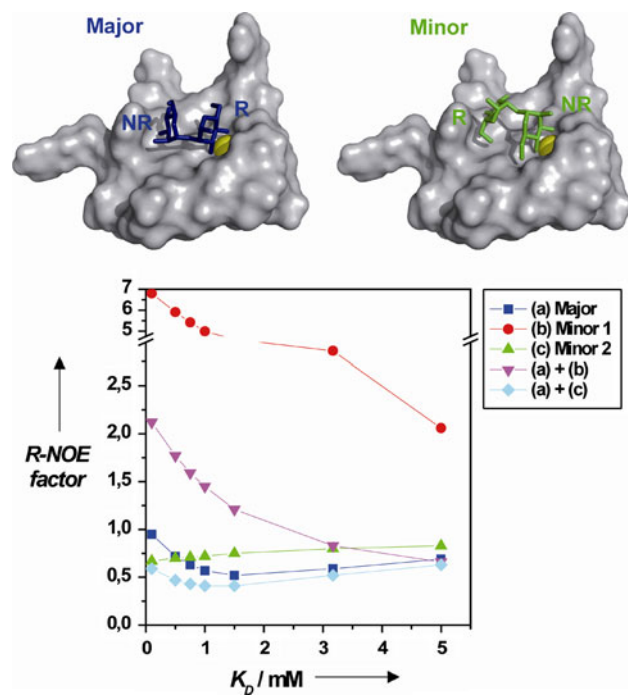

Fig. 10 Two binding modes are involved in molecular recognition of the disaccharide Manα1,2Man by the lectin DC-SIGN in solution (Angulo et al. 2008). STD NMR enabled elucidation of which modes contribute to the equilibrium. The *bottom curves* represent the "experimental-theoretical" fitting value (R-NOE) as a function of K_D for the different modes of interaction. The best fit with experimental data was obtained by a 75:25 equilibrium (*cyan*) of Major (*blue*) and Minor2 (*green*)

Fig. 11 The human monoclonal anti-HIV-1 antibody recognizes alternative binding modes of a branched pentamannoside in which both ends (D2 and D3) of the ligand compete for the same binding pocket (Enríquez-Navas et al. 2011). *Bottom left*: experimental STD build-up curves. *Bottom right*: theoretical STD curves (calculated from CORCEMA-ST) for a dual binding equilibrium (D2 + D3). Neither of the single binding modes (D2 or D3) alone was able to explain the experimental observations
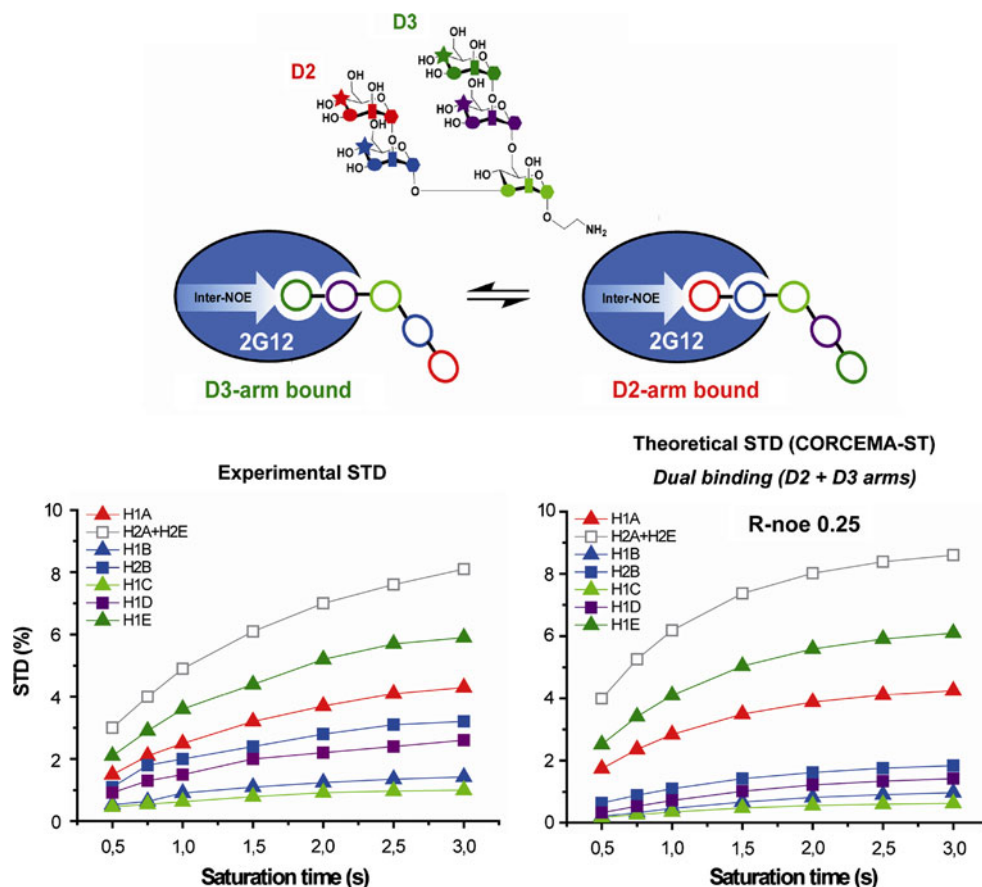
Analysis of multiple binding modes

The case of multiple binding modes of the same ligand in a single binding site can be considered as a special case of a competitive inhibition assay, in which one binding mode serves as inhibitor of all others. Because ligand and inhibitor(s) are the same species, chemical shifts and equilibrium intensities of their signals are equivalent and indistinguishable. Therefore, the total saturation observed in an STD experiment would be the addition of the accumulated saturations for each binding mode.

$$L + P \rightleftharpoons LP_1 + LP_2 + \cdots + LP_i + \cdots + Lp_n.$$

Even if we were able to evaluate the individual contributions of each species, the simple addition expressed in the equation above may not always apply, because it implicitly assumes that each term only contains structural information on a given binding mode. However, if the fraction of bound ligand was large enough, as explained above, the probability of fast ligand rebinding would be significant. Moreover, there would be processes of fast ligand "cross-rebinding", in which a ligand previously bound in a binding mode "*i*" returns to the binding pocket in a different binding mode "*j*" without

having relaxed back to equilibrium. In this way, the different contributions to the macroscopic STD intensities would become mixed, making it impossible to reduce the experimental observation to a simple sum of the different terms.

For the same reasoning as before, the solution to this problem lies in the use of initial STD build-up slopes around $t_{sat} = 0$ where no rebinding is possible. If we can calculate theoretical initial slopes for each expected binding mode (using CORCEMA-ST), the experimental initial STD slope can be expressed as their sum:

$$STD_0(\text{multiple} - \text{binding})$$
$$= \frac{I_0 - I_{sat}^{exp}}{I_0}\bigg|_{t_{sat}\to 0} = \frac{\sum_i (I_0 - I_{sat}^i)}{I_0}\bigg|_{t_{sat}\to 0} = \sum_i STD_0^i$$

Thus, if a number of structural models for the given protein–ligand complex are available (e.g., from X-ray, docking, etc.), and no single model is able to reproduce the experimental STD NMR data, combinations of different models can be tried. The best fit, yielding a minimum R-NOE value for the initial STD slopes, will elucidate what binding modes contribute to the molecular recognition of the ligand by the protein receptor.

For the lectin DC-SIGN, an important surface receptor in dendritic cells and participant in HIV infection processes, the binding of a dimannoside was studied by X-ray crystallography, revealing a well-characterized major binding mode and the possibility that further ill-defined binding orientations of the ligand contribute to an affinity enhancement. By STD NMR, and following the described approach of CORCEMA-ST prediction of initial STD build-up slopes, it was possible to elucidate the orientation of the ligand in the second binding mode (Fig. 10), showing that there is a change in the "reducing-to-non-reducing" orientation of the disaccharide when changing between binding modes (Angulo et al. 2008).

In another example on the molecular recognition of a branched pentamannoside by the human monoclonal anti-HIV-1 antibody 2G12, CORCEMA-ST analysis of initial STD build-up rates led to the conclusion that both arms of the biantennary ligand are competing for the same binding pocket with similar affinity, resulting in alternative binding modes (Fig. 11) (Enríquez-Navas et al. 2011).

Conclusions

Careful analysis of STD data can afford a wealth of information about the local structure of transient biomolecular complexes, particularly description of the interface and contacts between ligand and receptor. Initial qualitative applications of STD-NMR include the screening of small ligand libraries, or mapping of their binding epitope by comparison of relative STD intensities. Initial semi-quantitative applications assumed that the relative intensities of different signals do not depend on the saturation time, which is not true. Therefore, accurate quantification requires cancellation of the effects of relaxation and/or rebinding on the STD build-up, which applies at the limit of zero saturation time (yielding the initial slope of the STD amplification factor, $STD\text{-}AF_0$). More precise analysis can be achieved by comparing experimental and theoretical $STD\text{-}AF_0$ values, leading to the possibility of deducing more precise geometrical information. Although this method suffers from the need for preliminary structural models to calculate theoretical values by CORCEMA, it has been used satisfactorily in several cases, including examples of multiple binding modes.

References

Angulo J, Langpap B, Blume A, Biet T, Meyer B, Krishna NR, Peters H, Palcic MM, Peters T (2006) Blood group B galactosyltransferase: insights into substrate binding from NMR experiments. J Am Chem Soc 128:13529–13538

Angulo J, Díaz I, Reina JJ, Tabarani G, Fieschi F, Rojo J, Nieto PM (2008) Saturation transfer difference (STD) NMR spectroscopy characterization of dual binding mode of a mannose disaccharide to DC-SIGN. ChemBioChem 9:2225–2227

Angulo J, Enríquez-Navas PM, Nieto PM (2010) Ligand-receptor binding affinities from saturation transfer difference (STD) NMR spectroscopy: the binding isotherm of STD initial growth rates. Chem Eur J 16:7803–7812

Assadi-Porter FM, Tonelli M, Maillet E, Hallenga K, Benard O, Max M, Markley JL (2008) Direct NMR detection of the binding of functional ligands to the human sweet receptor, a heterodimeric family 3 GPCR. J Am Chem Soc 130:7212–7213

Bernardi A, Arosio D, Potenza D, Sánchez-Medina I, Mari S, Cañada FJ, Jiménez-Barbero J (2004) Intramolecular carbohydrate—aromatic interactions and intermolecular van der waals interactions enhance the molecular recognition ability of GM1 glycomimetics for cholera toxin. Chem Eur J 10:4395–4406

Blobel J, Fayos R, García J, Marimon O, Pérez Y, Pons M (2008) Low-molecular-weight spies of protein–protein interactions. Comptes Rendus Chimie 11:499–505

Calarese DA, Scanlan CN, Zwick MB, Deechongkit S, Mimura Y, Kunert R, Zhu P, Wormald MR, Stanfield RL, Roux KH, Kelly JW, Rudd PM, Dwek RA, Katinger H, Burton DR, Wilson IA (2003) Antibody domain exchange is an immunological solution to carbohydrate cluster recognition. Science 300:2065–2071

Calarese DA, Lee HK, Huang CY, Best MD, Astronomo RD, Stanfield RL, Katinger H, Burton DR, Wong CH, Wilson IA (2005) Dissection of the carbohydrate specificity of the broadly neutralizing-anti-HIV-1 antibody 2G12. Proc Natl Acad Sci USA 102:13372–13377

Calle LP, Canada FJ, Jimenez-Barbero J (2011) Application of NMR methods to the study of the interaction of natural products with biomolecular receptors. Nat Prod Rep 28:1118–1125

Canales A, Matesanz R, Gardner NM, Andreu JM, Paterson I, Díaz JF, Jiménez-Barbero J (2008) The bound conformation of microtubule-stabilizing agents: NMR insights into the bioactive 3D structure of discodermolide and dictyostatin. Chem Eur J 14:7557–7569

Caraballo R, Dong H, Ribeiro JP, Jimenez-Barbero J, Ramstrom O (2010) Direct STD NMR identification of beta-galactosidase inhibitors from a virtual dynamic hemithioacetal system. Angewandte Chemie-Int Ed 49:589–593

Claasen B, Axmann M, Meinecke R, Meyer B (2005) Direct observation of ligand binding to membrane proteins in living cells by a saturation transfer double difference (STDD) NMR spectroscopy method shows a significantly higher affinity of integrin alpha(IIb)beta(3) in native platelets than in liposomes. J Am Chem Soc 127:916–919

Di Micco S, Bassarello C, Bifulco G, Riccio R, Gomez-Paloma L (2006) Differential-frequency saturation transfer difference NMR spectroscopy allows the detection of different ligand-DNA binding modes. Angew Chem Int Ed 45:224–228

Diercks T, Ribeiro JP, Cañada FJ, André S, Jiménez-Barbero J, Gabius H-J (2009) Fluorinated carbohydrates as lectin ligands: versatile sensors in 19F-detected saturation transfer difference NMR spectroscopy. Chem Eur J 15:5666–5668

Enríquez-Navas PM, Marradi M, Padro D, Angulo J, Penadés S (2011) A solution NMR study of the interactions of oligomannosides and the

anti-HIV-1 2G12 antibody reveals distinct binding modes for branched ligands. Chem Eur J 17:1547–1560

Feher K, Groves P, Batta G, Jimenez-Barbero J, Muhle-Goll C, Kover KE (2008) Competition saturation transfer difference experiments improved with isotope editing and filtering schemes in NMR-based screening. J Am Chem Soc 130:17148–17153

Forsen S, Hoffman RA (1963) Study of moderately rapid chemical exchange reactions by means of nuclear magnetic double resonance. J. Chem. Phys. 39:2892 –2901

Haselhorst T, Munster-Kuhnel AK, Oschlies M, Tiralongo J, Gerardy-Schahn R, von Itzstein M (2007) Direct detection of ligand binding to sepharose-immobilised protein using saturation transfer double difference (STDD) NMR spectroscopy. Biochem Biophys Res Commun 359:866–870

Haselhorst T, Garcia JM, Islam T, Jimmy CC, Lai Faith J, Rose John M, Nicholls JS, Malik P, von Itzstein M (2008) Avian influenza H5-containing virus-like particles (VLPs): host-cell receptor specificity by STD NMR spectroscopy. Angew Chem Int Ed 47:1910–1912

Huang H, Milojevic J, Melacini G (2008) Analysis and optimization of saturation transfer difference NMR experiments designed to map early self-association events in amyloidogenic peptides. J Phys Chem B 112:5795–5802

Hyde EI, Birdsall B, Roberts GCK, Feeney J, Burgen ASV (1980) Proton nuclear magnetic resonance saturation transfer studies of coenzyme binding to lactobacilus-casei dihydrofolate-reductase Biochemistry 19:3738–3746

Jayalakshmi V, Krishna NR (2002) Complete relaxation and conformational exchange matrix (CORCEMA) analysis of intermolecular saturation transfer effects in reversibly forming ligand-receptor complexes. J Magn Reson 155:106–118

Jayalakshmi V, Krishna NR (2004) CORCEMA refinement of the bound ligand conformation within the protein binding pocket in reversibly forming weak complexes using STD-NMR intensities. J Magn Reson 168:36–45

Jayalakshmi V, Krishna NR (2005) Determination of the conformation of trimethoprim in the binding pocket of bovine dihydrofolate reductase from a STD-NMR intensity-restrained CORCEMA-ST optimization. J Am Chem Soc 127:14080–14084

Jayalakshmi V, Biet T, Peters T, Krishna NR (2004) Refinement of the conformation of UDP-galactose bound to galactosyltransfer-ase using the STD NMR intensity-restrained CORCEMA optimization. J Am Chem Soc 126:8610–8611

Jimenez-Barbero J, Peters T (2002) NMR spectroscopy of glycoconjugates. VCH, Weinheim

Kover KE, Groves P, Jimenez-Barbero J, Batta G (2007) Molecular recognition and screening using a N-15 group selective STD NMR method. J Am Chem Soc 129:11579–11582

Kover KE, Weber E, Martinek TA, Monostori E, Batta G (2010) N-15 and C-13 group-selective techniques extend the scope of STD NMR detection of weak host-guest interactions and ligand screening. ChemBioChem 11:2182–2187

Lepre CA, Moore JM, Peng JW (2004) Theory and applications of NMR-based screening in pharmaceutical research. Chem Rev 104:3641–3675

Maaheimo H, Kosma P, Brade L, Brade H, Peters T (2000) Mapping the binding of synthetic disaccharides representing epitopes of chlamydial lipopolysaccharide to antibodies with NMR. Biochemistry 39:12778–12788

Mari S, Serrano-Gomez D, Canada FJ, Corbi AL, Jimenez-Barbero J (2005) 1D saturation transfer difference NMR experiments on living cells: the DC-SIGN/oligomannose interaction. Angew Chem Int Ed 44:296–298

Martin JN, Munoz EM, Schwergold C, Souard F, Asensio JL, Jimenez-Barbero J, Canada J, Vicent C (2005) Carbohydrate-based DNA ligands: sugar-oligoamides as a tool to study carbohydrate—nucleic acid interactions. J Am Chem Soc 127:9518–9533

Mayer M, James TL (2002) Detecting ligand binding to a small RNA target via saturation transfer difference NMR experiments in D2O and H2O. J Am Chem Soc 124:13376–13377

Mayer M, James TL (2004) NMR-based characterization of phenothiazines as a RNA binding scaffold. J Am Chem Soc 126: 4453–4460

Mayer M, Meyer B (1999) Characterization of ligand binding by saturation transfer difference NMR spectroscopy. Angewandte Chemie-Int Ed 38:1784–1788

Mayer M, Meyer B (2001) Group epitope mapping by saturation transfer difference NMR to identify segments of a ligand in direct contact with a protein receptor. J Am Chem Soc 123: 6108–6117

Megy S, Bertho G, Gharbi-Benarous J, Evrard-Todeschi N, Coadou G, Segeral E, Iehle C, Quemeneur E, Benarous R, Girault JP (2005) STD and TRNOESY NMR studies on the conformation of the oncogenic protein beta-catenin containing the phosphorylated motif DpSGXXpS bound to the beta-TrCP protein. J Biol Chem 280:29107–29116

Meyer B, Peters T (2003) NMR Spectroscopy techniques for screening and identifying ligand binding to protein receptors. Angewandte Chemie-Int Ed 42:864–890

Moseley HNB, Curto EV, Krishna NR (1995) Complete relaxation and conformational exchange matrix (CORCEMA) analysis of NOESY spectra of interacting systems; two-dimensional transferred NOESY. J Magn Reson Ser B, 108:243–261

Neffe AT, Bilang M, Meyer B (2006) Synthesis and optimization of peptidomimetics as HIV entry inhibitors against the receptor protein CD4 using STD NMR and ligand docking. Org Biomol Chem 4:3259–3267

Neffe AT, Bilang M, Gruneberg I, Meyer B (2007) Rational optimization of the binding affinity of CD4 targeting peptidomimetics with potential anti HIV activity. J Med Chem 50:3482–3488

Neuhaus D, Williamson MP (2000) The nuclear overhauser effect in structural and conformational analysis. Wiley-VCH, New York

Pellecchia M, Sem DS, Wuthrich K (2002) NMR in drug discovery. Nat Rev Drug Discov 1:211–219

Pellecchia M, Bertini I, Cowburn D, Dalvit C, Giralt E, Jahnke W, James TL, Homans SW, Kessler H, Luchinat C, Meyer B, Oschkinat H, Peng J, Schwalbe H, Siegal G (2008) Perspectives on NMR in drug discovery: a technique comes of age. Nat Rev Drug Discov 7:738–745

Peñalver P, Marcelo F, Jiménez-Barbero J, Vicent C (2011) Carbohydrate recognition at the minor-groove of the self-complementary duplex d(CGCGAATTCGCG)2 by a synthetic glyco-oligoamide. Chem Eur J 17:4561–4570

Pereira A, Pfeifer TA, Grigliatti TA, Andersen RJ (2009) Functional cell-based screening and saturation transfer double-difference NMR have identified haplosamate a as a cannabinoid receptor agonist. ACS Chem Biol 4:139–144

Rademacher C, Peters T (2008) Molecular recognition of ligands by native viruses and virus-like particles as studied by NMR experiments. In: Peters T (ed) Bioactive conformation II, vol 273. Springer, Berlin/Heidelberg, pp 183–202

Rademacher C, Krishna NR, Palcic M, Parra F, Peters T (2008) NMR experiments reveal the molecular basis of receptor recognition by a calicivirus. J Am Chem Soc 130:3669–3675

Rademacher C, Guiard J, Kitov PI, Fiege B, Dalton KP, Parra F, Bundle DR, Peters T (2011) Targeting norovirus infection—multivalent entry inhibitor design based on NMR experiments. Chem Eur J 17:7442–7453

Räuber C, Berger S (2010) 13C-NMR detection of STD spectra. Magn Reson Chem 48:91–93

Ribeiro JP, André S, Cañada FJ, Gabius H-J, Butera AP, Alves RJ, Jiménez-Barbero J (2010) Lectin-based drug design: combined strategy to identify lead compounds using STD NMR spectroscopy, solid-phase assays and cell binding for a plant toxin model. Chem Med Chem 5:415–419

Roldós V, Cañada FJ, Jiménez-Barbero J (2011) Carbohydrate–protein interactions: a 3D view by NMR. ChemBioChem 12:990–1005

Souard F, Muñoz E, Peñalver P, Badía C, del Villar-Guerra R, Asensio JL, Jiménez-Barbero J, Vicent C (2008) Sugar—oligoamides: bound-state conformation and DNA minor-groove-binding description by TR-NOESY and differential-frequency saturation-transfer-difference experiments. Chem Eur J 14:2435–2442

Vogtherr M, Peters T (2000) Application of NMR based binding assays to identify key hydroxy groups for intermolecular recognition. J Am Chem Soc 122:6093–6099

Wagstaff JL, Vallath S, Marshall JF, Williamson RA, Howard MJ (2010) Two-dimensional heteronuclear saturation transfer difference NMR reveals detailed integrin alpha v beta 6 protein-peptide interactions. Chem Commun 46:7533–7535